SEMARAK ILMU PUBLISHING

Journal of Advanced Research in Fluid Mechanics and Thermal Sciences

Journal homepage:
https://semarakilmu.com.my/journals/index.php/fluid_mechanics_thermal_sciences/index
ISSN: 2811-3950

Aligned Magnetohydrodynamics Free Convection Flow of Magnetic Nanofluid over a Moving Vertical Plate with Convective Boundary Condition

Nor Alifah Rosaidi[1], Nurul Hidayah Ab Raji[1,*], Siti Nur Hidayatul Ashikin Ibrahim[1], Mohd Rijal Ilias[2]

[1] Universiti Teknologi MARA Cawangan Perlis, Kampus Arau, 02600 Arau, Perlis, Malaysia
[2] Universiti Teknologi MARA Shah Alam, 40450 Shah Alam, Selangor, Malaysia

ARTICLE INFO

Article history:
Received 17 July 2021
Received in revised form 29 January 2022
Accepted 31 January 2022
Available online 18 March 2022

Keywords:
Aligned MHD; Convective Boundary Condition; Moving Vertical Plate

ABSTRACT

Due to its substantial applications in physics, chemistry, and engineering, some emphasis has been given in recent years to explore the boundary layer flow of magnetohydrodynamic (MHD) nanofluids. The numerical study is conducted to investigate the behaviour of MHD free convection flow of magnetic nanofluids over a moving vertical plate with convective boundary conditions by taking a few types of parameters into consideration. The similarity transformation was used to reduce the partial differential governing equations into ordinary differential equations. Then, the reduced equations were solved using fourth-fifth order Runge–Kutta–Fehlberg and coded into Maple Software. The results of velocity and temperature profiles were illustrated graphically while the results of skin friction coefficient and Nusselt number were presented in tabulated data. As a result, inclination angle of magnetic field parameter, magnetic interaction parameter, Grashof number and Biot number improve the velocity field and lowers the momentum boundary layer thickness. However, the nanoparticle volume fraction parameter, and the Biot number parameter boost the temperature field and raise the thermal boundary layer thickness. The Nusselt number of the moving plate with the flow is the highest, whereas the skin friction coefficient of the moving plate against the flow is the highest. Fe_3O_4-kerosene has a better influence to the velocity and temperature profiles as well as skin friction coefficient and Nusselt number.

1. Introduction

Magnetic nanofluids or known as ferrofluids, are the colloidal dispersion of magnetic particles that are nanometer sized [1]. Based on the coated surface, the ferrofluids can be identified as surfaced ferrofluids or ionic ferrofluids. The magnetic nanofluids are also known as a heat carrier and widely used in various fields. Hence, intensive studies on the behaviours of magnetic nanofluids have been done by most of researchers, whose are interested to analyses the problems that are related to heat transfer due to their eager to find the solution for this problem. Magnetic nanofluids were

* *Corresponding author.*
E-mail address: hidayah417@uitm.edu.my

https://doi.org/10.37934/arfmts.93.2.3749

suggested as alternatives since they were more cost-effective and offered superior heat transfer improvements. Many studies have been done by considering various types of plates and boundary conditions [2-8].

Most of the researchers conduct their study based on free convection flow fluid because it is easier to analyses the behaviours of the magnetic nanofluids since it naturally occurs without influenced by any external forces. Previous study by Illias *et al.,* [9,10] investigated unsteady aligned MHD boundary layer flow and heat transfer of a magnetic nanofluids past a vertical plate and an inclined plate. They discovered that the Grashof number has a considerable impact on the velocity and momentum boundary layer thickness. Magnetic nanofluids, Fe_3O_4-kerosene and Fe_3O_4-water exhibited a significant improvement in heat transfer rate and skin friction coefficient compared to Al_2O_3-kerosene and Al_2O_3-water.

Recently, researchers are interested to conduct a study on the convective boundary condition since this boundary condition is one of the problems that are related to heat transfer and usually happens in daily life. Makinde and Aziz [11] and Yao *et al.,* [12] investigated the effect of convective boundary condition on boundary layer flow, heat transfer and nanoparticle fraction over a stretching or shrinking surface in a nanofluid and viscous fluid with restricted for two boundary condition which is prescribed temperatures or heat flux for heat transfer characteristics. When the Biot number approaches infinity, the convective boundary condition affects the velocity and temperature profiles, and both problems are reduced to a constant wall temperature boundary condition. Several authors investigate the influences of convective boundary condition and induced magnetic field on MHD stagnation point flow over a stretching sheet [13-15]. Goyal and Bhargava [16] and Mitra [17] also used a convective boundary condition to study the boundary layer flow of a nanofluid over a convective heated inclined plate.

MHD is the phenomena that occur when a magnetic field is applied to an electrically conducting fluid. In recent years, research in the field of MHD has progressed quickly. The study of flow and heat transfer when a magnetic field is applied past a heated surface yielded many applications involving an electrically conducting fluid. Ilias *et al.,* [18] analyses the influences of convective boundary condition on the magnetic nanofluids over a flat vertical plate with the presence of a magnetic field and continues the researches by considering the inclined plate [19]. They discovered that aligned magnetic field parameter influence the total magnetic interaction parameter. The value of the aligned magnetic field has a huge impact on velocity, temperature, skin friction coefficient, and Nusselt number. There are several studies in MHD recently [20-26].

However, to the extent of authors' knowledge, the study on convective boundary condition is mostly conducted on a plate with static position. Thus, this study is aimed to investigate the behaviour of aligned MHD free convection flow of magnetic nanofluids over a moving vertical plate with convective boundary condition by analysing the velocity and temperature profiles as well as the numerical results on the skin friction coefficient and Nusselt number.

2. Mathematical Formulation

This study considers a steady state of two-dimensional laminar free convection boundary layer flow of a magnetic nanofluids flow over a moving vertical plate in the presence of aligned magnetic field. The aligned magnetic field, α was introduced to the flow and placed in the free stream temperature T_∞**.** The mixtures of magnetic nanofluids used in this study were Fe_3O_4-water and Fe_3O_4-kerosene. The transverse magnetic field assumed to be a function of the distance from the origin and can be expressed as $B(x)=B_0/\sqrt{x}$ where $B_0 \neq 0$.

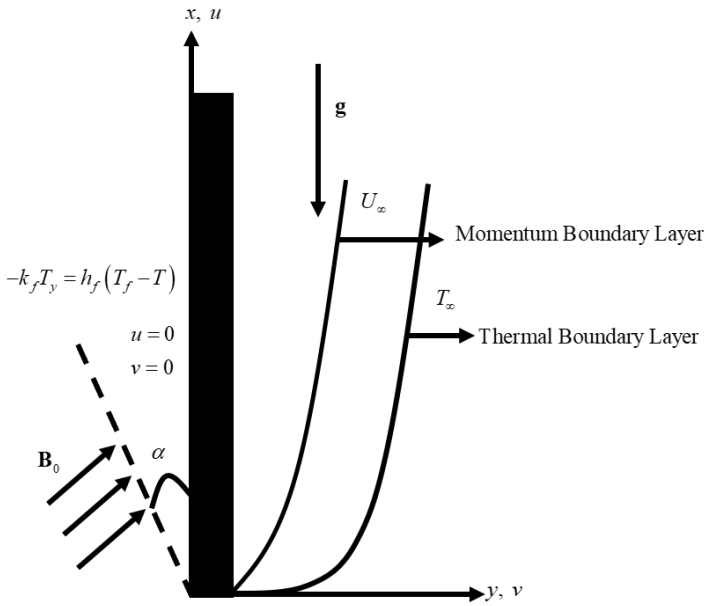

Fig. 1. Physical model and coordinate system of the experiment [18]

Here, B_0 represent the strength of magnetic field and the coordinate (x, y) along the plate respectively. The base fluids and nanoparticles are in thermal equilibrium and no slip occurs between them. The spherical shaped nanoparticles are considered. The viscous dissipation and radiation are neglected in the analysis.

Together with assumptions of Boussinesq and boundary layer approximations, the governing equations of MHD boundary layer flow can be expressed as [18]:

$$u_x + v_y = 0 \tag{1}$$

$$uu_x + vu_y = \frac{\mu_{nf}}{\rho_{nf}} u_{yy} + \frac{(\rho\beta)_{nf}}{\rho_{nf}} g\left(T - T_\infty\right) - \frac{\sigma B^2(x)}{\rho_{nf}} \sin^2\alpha\left(u - U_\infty\right) \tag{2}$$

$$uT_x + vT_y = \alpha_{nf} T_{yy} \tag{3}$$

While the boundary conditions used in this study are as follows:

$$\begin{aligned} &u = \varepsilon U_\infty,\ v = 0,\ -kT_y = h_f\left[T_f - T\right] \text{ at } y = 0 \\ &u = U_\infty,\ T = T_\infty \text{ as } y \to \infty \end{aligned} \tag{4}$$

where u and v are refers to x (along the plate) and y (normal to the plate) components of velocity respectively. T is the temperature of magnetic nanofluids, h_f is the heat transfer coefficient of the plate, and T_f is the temperature of the hot fluids at the left plate surface convectively heating the plate. Besides, U_∞ is the constant free stream velocity while σ is the electrical conductivity. The effective properties of magnetic nanofluids may be expressed in terms of the properties of base fluids, nanoparticles and the volume fraction of solid nanoparticles as follow [27].

$$\rho_{nf}=(1-\phi)\rho_f+\phi\rho_s,$$
$$\left(\rho C_p\right)_{nf}=(1-\phi)\left(\rho C_p\right)_f+\phi\left(\rho C_p\right)_s,\quad (\rho\beta)_{nf}=(1-\phi)(\rho\beta)_f+\phi(\rho\beta)_s, \tag{5}$$
$$\mu_{nf}=\frac{\mu_f}{(1-\phi)^{2.5}},\quad \alpha_{nf}=\frac{k_{nf}}{\left(\rho C_p\right)_{nf}},\quad \frac{k_{nf}}{k_f}=\frac{k_s+2k_f-2\phi\left(k_f-k_s\right)}{k_s+2k_f+\phi\left(k_f-k_s\right)}$$

where ρ_{nf} is the effective density, ϕ is the solid volume fraction, ρ_f and ρ_s are the densities of pure fluid and nanoparticles respectively while μ_f and μ_{nf} are the dynamic viscosity of the base fluids and the effective dynamic viscosity respectively, $\left(\rho C_p\right)_{nf}$ is indicate the heat capacity of the magnetic nanofluids meanwhile the specific heat parameters of the base fluids and nanoparticles are denoted by $\left(\rho C_p\right)_f$ and $\left(\rho C_p\right)_s$ respectively, $(\rho\beta)_{nf}$ is the thermal expansion coefficient, α_{nf} is the thermal diffusivity of the magnetic nanofluids, k_{nf} is the thermal conductivity of the magnetic nanofluids, k_f and k_s are the thermal conductivities of the fluids and nanoparticles. The thermophysical properties of the base fluid and the solid nanoparticles are given in Table 1.

Table 1
Thermophysical properties of base fluids and ferroparticle [18]

Physical properties	Water	Kerosene	Fe_3O_4
$\rho(kg/m^3)$	997.1	780	5200
$C\,(J/kgK)$	4179	2090	670
$k\,(W/mK)$	0.613	0.149	6
$\beta\times10^{-5}\left(K^{-1}\right)$	21	99	1.3

The continuity equation in Eq. (1) is satisfied by the introducing stream function $\psi(x,y)$ as shown below,

$$u=\psi_y \text{ and } v=-\psi_x \tag{6}$$

The following similarity variables are introduced to solve the governing equations in Eq. (1) to Eq. (3), as in the study by Illias *et al.,* [18],

$$\eta=y\sqrt{\frac{U_\infty}{v_f x}}=\frac{y}{x}\sqrt{\mathrm{Re}_x},\ \psi=v_f\sqrt{\mathrm{Re}_x}\,f(\eta),\ \theta=\frac{T-T_\infty}{T_f-T_\infty} \tag{7}$$

where η is the similarity variable, $\mathrm{Re}_x=U_\infty x/v_f$ refer to Reynolds number, $f(\eta)$ and $\theta(\eta)$ indicates the non–dimensional stream function and temperature respectively.

By substitute Eq. (5), Eq. (6) and Eq. (7) into Eq. (2) and Eq. (3), the following nonlinear systems of ordinary differential equations were obtained:

$$f'''+(1-\phi)^{2.5}\left((1-\phi)+\phi\left(\frac{\rho_s}{\rho_f}\right)\right)\frac{1}{2}ff''$$
$$+(1-\phi)^{2.5}\left((1-\phi)+\phi\left(\frac{(\rho\beta)_s}{(\rho\beta)_f}\right)\right)Gr_x\theta+(1-\phi)^{2.5}M\left(1-f'\right)\sin^2\alpha=0 \quad (8)$$

$$\left(\frac{k_{nf}}{k_f}\right)\theta''+\frac{\Pr}{2}\left(1-\phi+\phi\left(\frac{(\rho C_p)_s}{(\rho C_p)_f}\right)\right)f\theta'=0 \quad (9)$$

By respecting to Eq. (4), the boundary conditions obtained were as follow:

$$f'(\eta)=\varepsilon,\ f(\eta)=0,\ \theta'(\eta)=-Bi_x\left(1-\theta(\eta)\right) \text{ at } \eta=0$$
$$f'(\eta)=1,\ \theta(\eta)=0 \text{ as } \eta\to\infty \quad (10)$$

where primes denote differentiation with respect to η, $M=\frac{\sigma B_0^{\ 2}}{\rho U_\infty}$ is the magnetic interaction parameter, $Gr_x=\frac{g\beta_f\left(T_f-T_\infty\right)x}{U_\infty^{\ 2}}$ is the local Grashof number, $\Pr=\frac{\left(\mu C_p\right)}{k_f}$ is the Prandtl number and $Bi_x=\frac{h_f}{k_f}\sqrt{\frac{x\nu_f}{U_\infty}}$ is the local Biot number. In order to have a true similarity solution, the parameters Gr_x and Bi_x must be constant and independent of x. By assuming $\beta_f=ax^{-1}$ and $h_f=bx^{-\frac{1}{2}}$ where a and b are constants, therefore $Gr=\frac{ag\left(T_f-T_\infty\right)}{U_\infty^{\ 2}}$ and $Bi=\frac{b}{k_f}\sqrt{\frac{\nu_f}{U_\infty}}$ [18,27].

The discussions of numerical results are based on the skin friction coefficient, C_f at the surface of the plate and local Nusselt number, Nu_x which are defined as:

$$C_f=\frac{\tau_w}{\rho_f U_\infty^{\ 2}},\ Nu_x=\frac{xq_w}{k_f\left(T_f-T_\infty\right)} \quad (11)$$

where τ_w refer to the wall skin friction and q_w refer to the heat flux from the plate which given by:

$$\tau_w=\mu_{nf}\left(u_y\right)_{y=0},\quad q_w=-k_{nf}\left(T_y\right)_{y=0} \quad (12)$$

By substitute Eq. (7) and Eq. (12) into Eq. (11), the solutions obtained were as follow:

$$C_f\sqrt{\mathrm{Re}_x}=\frac{f''(0)}{(1-\phi)^{2.5}},\quad \frac{Nu_x}{(\mathrm{Re}_x)^{1/2}}=-\frac{k_{nf}}{k_f}\theta'(0) \quad (13)$$

3. Method of Solution

The nonlinear Eq. (8) and Eq. (9) cannot be solved analytically. The relatively robust computer algebra software Maple 20 is used to derive numerical solutions subject to the boundary conditions (10). This software uses a fourth-fifth order Runge–Kutta–Fehlberg method as default to solve boundary value problems numerically using the dsolve command.

The results of the current study were compared to the results of a previous study that employed the identical boundary condition to demonstrate the dependability of the numerical results produced and the consistency of the investigation. From Table 2, we can see that the data produce has a good agreement with the previous researchers.

Table 2
Comparison result of $\theta(0)$ for different values of Biot number, Bi_x when $\alpha = 0,\ M = 0,\ \Pr = 0.72,\ Gr_x = 0,\ 0.5$ and $\varepsilon = 0$

Bi_x	$M = 0,\ \Pr = 0.72,\ Gr_x = 0,\ K = 0$					$M = 0,\ \Pr = 0.72,$ $Gr_x = 0.5,\ K = 0$	
	Bataller	Aziz	Ishak *et al.,*	Ramesh *et al.,*	Present	Ramesh *et al.,*	Present
0.05	0.1446	0.1447	0.1446	0.1446	0.144660	0.1388	0.138810
0.1	-	0.2528	0.2527	0.2527	0.252756	0.2386	0.238622
0.2	0.4035	0.4035	0.4035	0.4035	0.403520	0.3774	0.377434
0.4	-	0.5750	0.5750	0.5750	0.575012	0.5398	0.539854
0.6	0.6699	0.6699	0.6699	0.6699	0.669914	0.6337	0.633763
0.8	-	0.7302	0.7301	0.7301	0.730168	0.6954	0.695454
1.0	0.7718	0.7718	0.7718	0.7718	0.771821	0.7392	0.739209
5	-	0.9441	0.9441	0.9441	0.944173	0.9323	0.932320
10	0.9712	0.9713	0.9712	0.9712	0.971285	0.9648	0.964825

4. Results and Discussion

The effect of various physical parameters on velocity, temperature, skin friction, and Nusselt number is presented using graphs and tables. For the base fluids, water and kerosene, the Prandtl numbers are taken to be 6.2 and 21, respectively. We fit the nondimensional values as follows for numerical computation, $\alpha = 90°$, $M = 1$, $\phi = 0.1$, $Gr_x = 0.1$ and $Bi_x = 0.1$ unless otherwise mentioned. In this study, $\varepsilon = 0$ $\varepsilon = 0$ denotes the static plate, $\varepsilon < 0$ denotes moving plate against the flow and $\varepsilon > 0$ denotes moving plate together with the flow.

Figure 2 to Figure 6 shows how velocity and temperature profiles change with different values of α, M, ϕ, Gr_x and Bi_x. While the numerical value of skin friction coefficient and Nusselt number for Fe_3O_4-water and Fe_3O_4-kerosene are shown in Table 3 and Table 4.

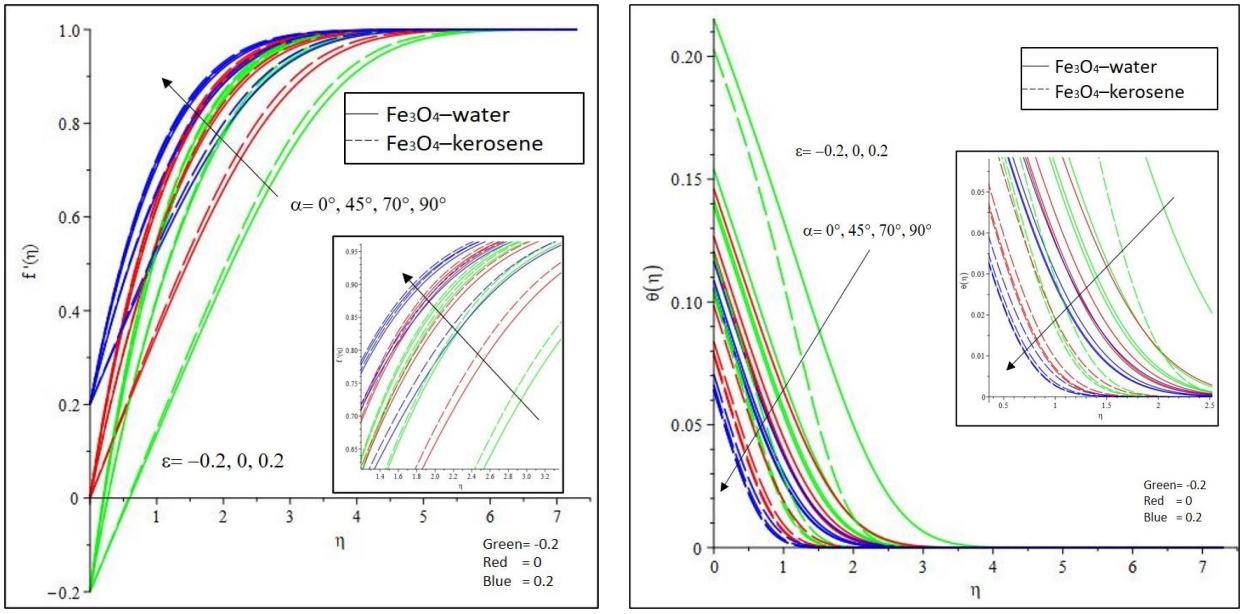

(a) (b)

Fig. 2. Effects of α on (a) velocity profiles and (b) temperature profiles

Figure 2(a) and Figure 2(b) depict the effects of α on the velocity and temperature profiles of Fe_3O_4-water and Fe_3O_4-kerosene magnetic nanofluids for $\varepsilon = -0.2$, $\varepsilon = 0$ and $\varepsilon = 0.2$. It shows that α has different influences on velocity and temperature profiles. For all three plate circumstances, as α increase the velocity profile increases while the temperature profile decreases. When $\alpha = 90°$, it corresponds to transverse magnetic field. As shown in Table 3 and Table 4, the skin friction coefficient and Nusselt number rise as α increases. In all states of plate, Fe_3O_4-kerosene has a greater skin friction coefficient than Fe_3O_4-water. However, at $\varepsilon = -0.2$ specifically at $\alpha = 0°$ and $45°$, Fe_3O_4-kerosene has a lower Nusselt number than Fe_3O_4-water.

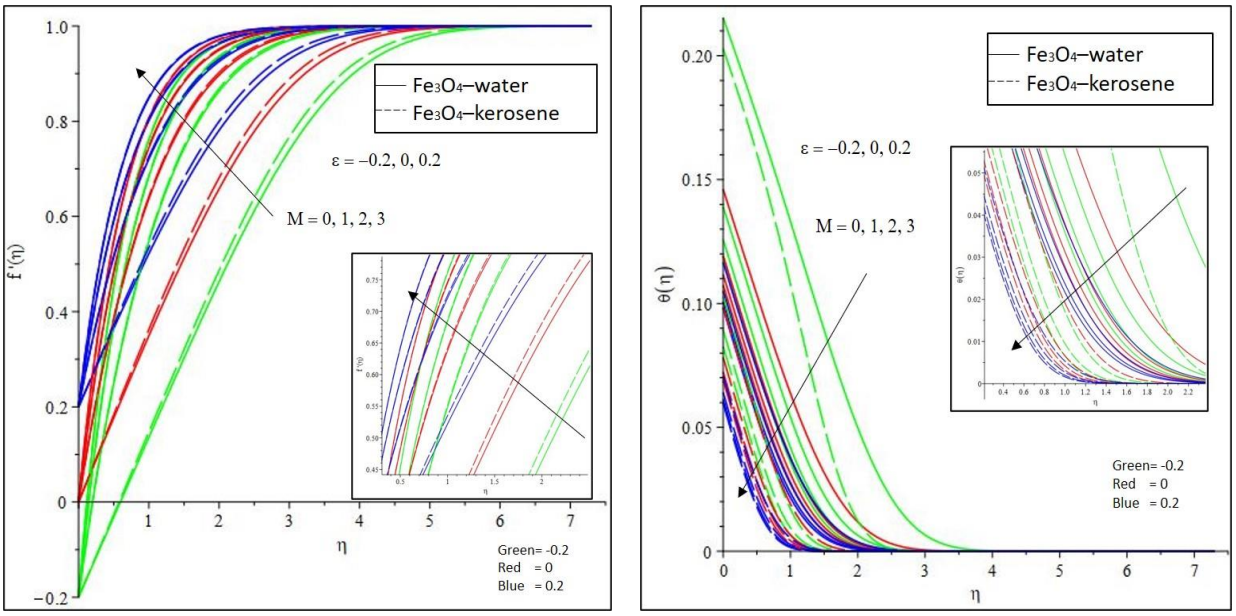

(a) (b)

Fig. 3. Effects of M on (a) velocity profiles and (b) temperature profiles

Figure 3(a) and Figure 3(b) illustrates the impact of M on velocity and temperature profiles at three different states of vertical plate. The strengthening in M causes the increasing in the velocity profiles while decreasing in the temperature profiles. The nanoparticles are generally arranged in order as the magnetic field increases. The magnetic field pushes the nanofluid, which is decelerated by the viscous force. This counteracts the viscous effects. As a result, as M is increased, the nanofluid's velocity increases, and the thickness of the momentum boundary layer decreases. $M = 0$ indicates the absence of magnetic field. For $\varepsilon = -0.2$, the temperature of Fe_3O_4-kerosene is initially higher than Fe_3O_4-water until at particular value η, the opposite characteristic occurs. M has a significant impact on skin friction coefficient and Nusselt number, as shown in Table 3 and Table 4. It occurs in all states of plate.

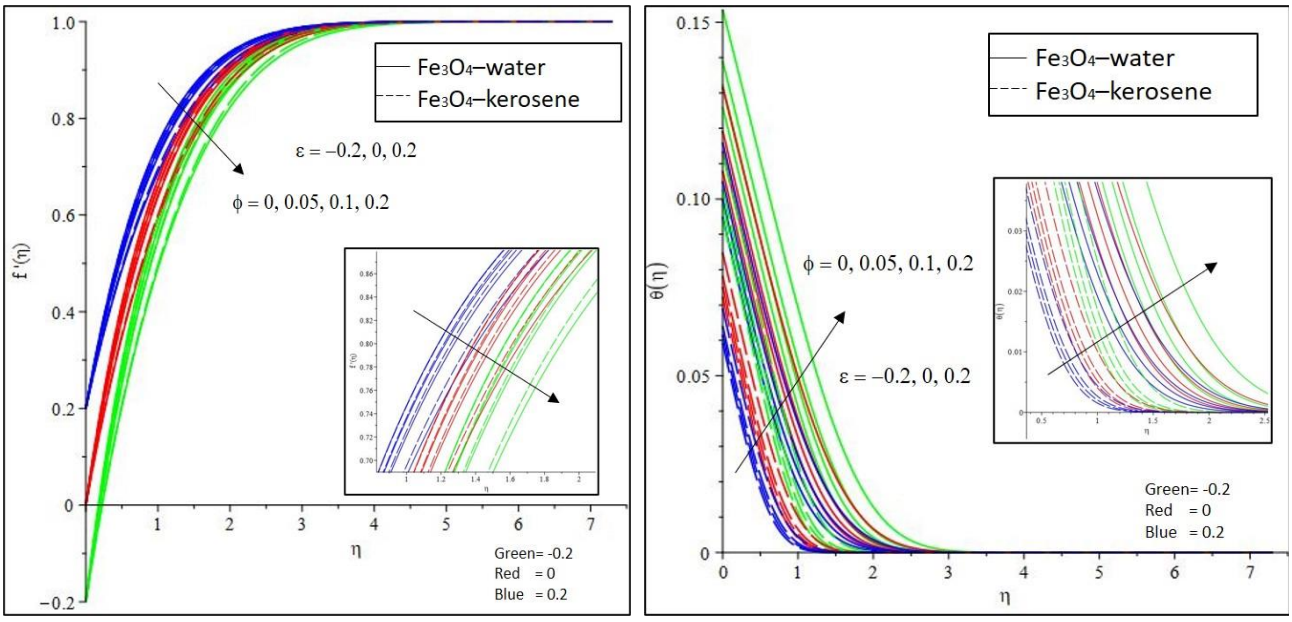

(a) (b)

Fig. 4. Effects of ϕ on (a) velocity profiles and (b) temperature profiles

The velocity profile decreased as ϕ increased, as seen in Figure 4(a), due to the significant frictional force between the magnetic nanoparticles and the plate surface. Momentum boundary layer increase for all cases. As shown in Figure 4(b), ϕ, on the other hand, improves the temperature profile by increasing the temperature as the magnetic nanoparticles collide with the plate's surface. The enhancement of magnetic nanofluids thermal conductivity is linked to the delicacy of the width of the thermal boundary layer by ϕ. To put it another way, the higher the thermal conductivity of a fluid, the higher the thermal diffusivity. A lower temperature gradient is caused by a higher value of thermal diffusivity. As a result, thermal boundary layer increases. This finding is consistent with the experimental findings described in a study by Xuan and Li [32]. Table 3 and Table 4 show that the skin friction coefficient and Nusselt number for both of Fe_3O_4-water and Fe_3O_4-kerosene rise as ϕ increases. At $\varepsilon = -0.2$, Fe_3O_4-water has a higher skin friction coefficient than Fe_3O_4-kerosene, whereas at $\varepsilon = 0$ and $\varepsilon = 0.2$, the converse is true. In all vertical plate states, Fe_3O_4-kerosene has greater value of Nusselt number than Fe_3O_4-water.

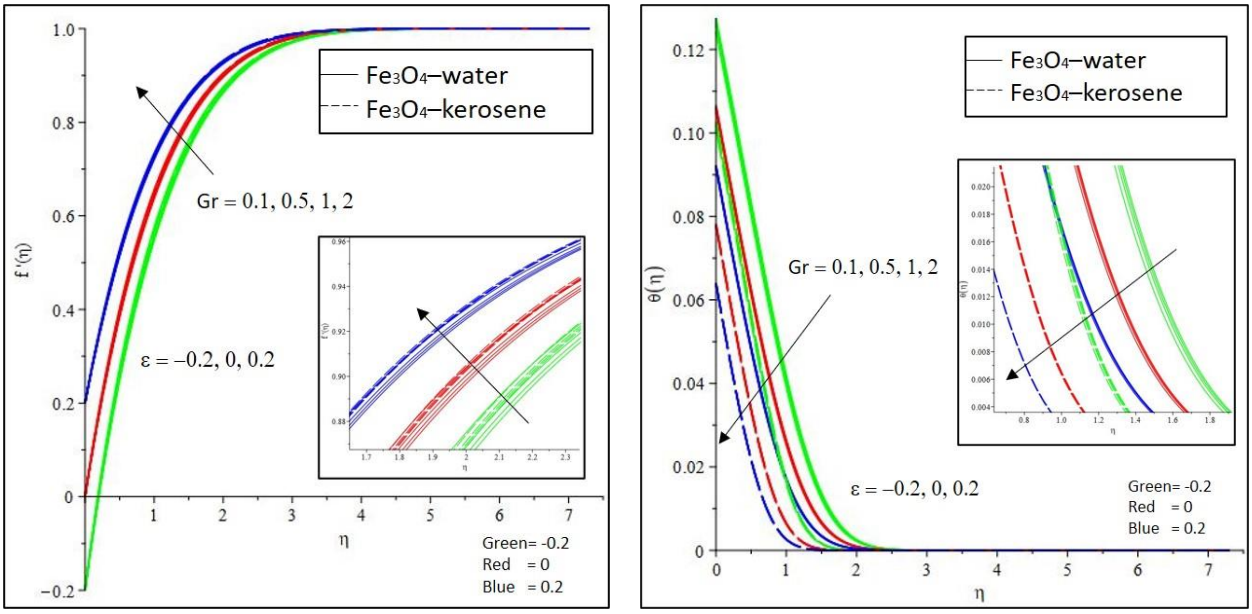

(a) (b)

Fig. 5. Effects of Gr_x on (a) velocity profiles and (b) temperature profiles

The effects of Gr_x on the velocity profiles is depicted in Figure 5(a). The velocity increased as Gr_x rose. Increases in Gr_x, on the other hand, diminish the temperature profiles, as shown in Figure 5(b). Because of the growing buoyancy effect on the magnetic nanofluids, the thickness of the momentum and thermal boundary layer decreases as the value of Gr_x increases. The rate of thermal diffusion within the boundary layer is slowed by the intensity of buoyant force. As shown in Table 3, increases in Gr_x increase the value of skin friction coefficient. The skin friction coefficient of Fe_3O_4-kerosene is the lowest when compared to Fe_3O_4-water at $\varepsilon = 0.2$. Table 4 demonstrates that as Gr_x increases, the Nusselt number increases only slightly, and the moving plate with flow has the maximum Nusselt number (Fe_3O_4-kerosene).

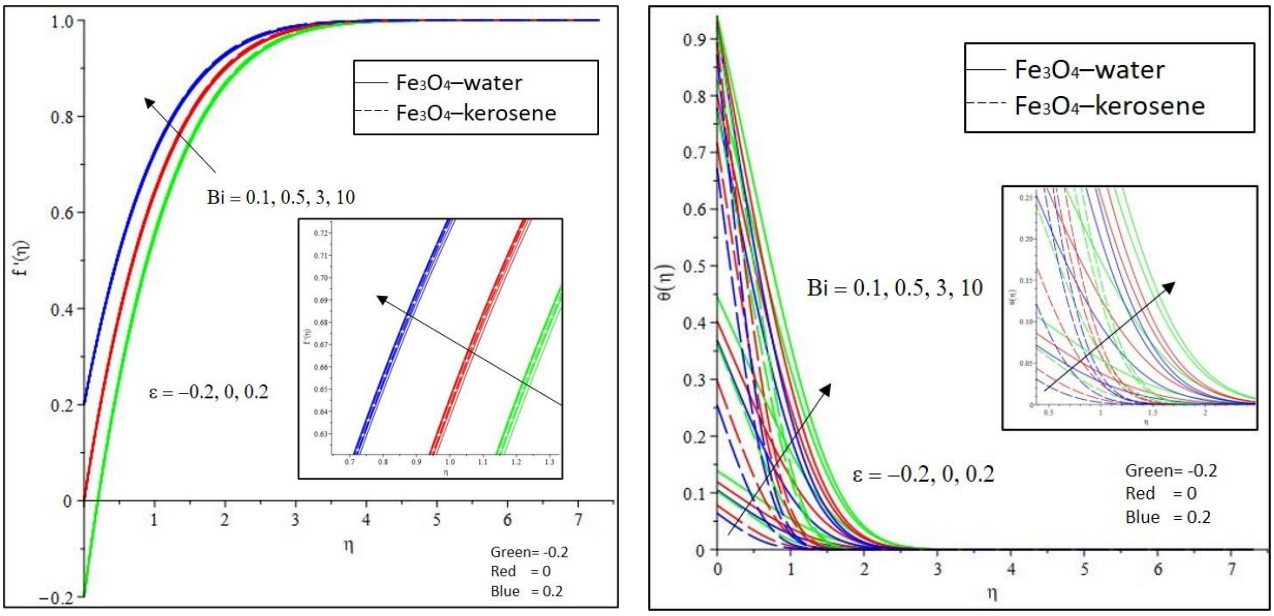

(a) (b)

Fig. 6. Effects of Bi_x on (a) velocity profiles and (b) temperature profiles

Based on Figure 6(a), Bi_x positively influences the velocity profiles in both mixtures of magnetic nanofluids. From the Table 3, the highest value of skin friction coefficient can be seen for the case of $\varepsilon = -0.2$ (Fe_3O_4-water). The effect of Bi_x on temperature diffusion is seen in Figure 6(b). Here $Bi_x \to \infty$ means a constant in the case of surface temperature. It's worth noting that as Bi_x rises, so does the temperature profile. Bi_x stands for the ratio of the hot fluid edge's convection resistance to the cold fluid edge's convection resistance over the surface. Furthermore, because hot fluid thermal resistance is proportional to h_f, increasing values of Bi_x coincides with a decrease in fluid edge convection. As a result, the thermal boundary layer's width increases. The heat transfer rate at the plate surface increases, as indicated in Table 4, especially in the case of $\varepsilon = 0.2$ (Fe_3O_4-kerosene).

Table 3
Variation in skin friction coefficient at different dimensionless parameters for Fe_3O_4-water and Fe_3O_4-kerosene

α	M	Gr_x	ϕ	Bi_x	Skin Friction Coefficient					
					Fe_3O_4-water			Fe_3O_4-kerosene		
					ε = -0.2	ε = 0	ε = 0.2	ε = -0.2	ε = 0	ε = 0.2
0°	1	0.1	0.1	0.1	0.4412	0.4636	0.43363	0.4548	0.4575	0.4293
45°					1.0546	0.9177	0.76471	1.0587	0.9141	0.7616
70°					1.3506	1.1551	0.94777	1.3533	1.1521	0.9451
90°					1.4290	1.2187	0.99728	1.4315	1.2158	0.9947
90°	0	0.1	0.1	0.1	0.4412	0.4636	0.4336	0.4548	0.4575	0.4393
	1				1.4290	1.2187	0.9973	1.4315	1.2158	0.9947
	2				1.9774	1.6676	1.3410	1.9790	1.6654	1.3479
	3				2.4045	2.0199	1.6289	2.4056	2.0180	1.6272
90°	1	0.1	0.1	0.1	1.4280	1.2177	0.9964	1.4315	1.2158	0.9947
		0.5			1.4525	1.2362	1.0109	1.4476	1.2271	1.0029
		1			1.4825	1.2590	1.0290	1.4675	1.2410	1.0130
		2			1.5407	1.3039	1.0648	1.5061	1.2685	1.0331
90°	1	0.1	0	0.1	1.2383	1.0489	0.8529	1.2357	1.0464	0.8507
			0.05		1.3279	1.1287	0.9207	1.3277	1.1295	0.9222
			0.1		1.4288	1.1287	0.9973	1.4315	1.2233	1.0029
			0.2		1.6748	1.4377	1.1836	1.6841	1.4517	1.1995
90°	1	0.1	0.1	0.1	1.4290	1.2187	0.9973	1.4315	1.2233	1.0029
				0.5	1.4448	1.2321	1.0088	1.4418	1.2306	1.0085
				3	1.4645	1.2509	1.0265	1.4579	1.2446	1.0205
				10	1.4703	1.2569	1.0328	1.4636	1.2504	1.0263

Table 4
Variation of Nusselt number at different dimensionless parameters for Fe_3O_4-water and Fe_3O_4-kerosene

α	M	Gr_x	ϕ	Bi_x	Nusselt number					
					Fe_3O_4-water			Fe_3O_4-kerosene		
					ε = -0.2	ε = 0	ε = 0.2	ε = -0.2	ε = 0	ε = 0.2
0°	1	0.1	0.1	0.1	0.0974	0.1060	0.1097	0.10421	0.11716	0.12096
45°					0.10504	0.1084	0.11065	0.11513	0.11926	0.1216
70°					0.10658	0.1092	0.11103	0.11692	0.11990	0.12186
90°					0.10690	0.1094	0.11112	0.11728	0.12005	0.12192
90°	0	0.1	0.1	0.1	0.0974	0.1060	0.1097	0.1172	0.1172	0.1210
	1				0.1069	0.1094	0.1111	0.1200	0.1200	0.1219
	2				0.1086	0.1103	0.1116	0.1209	0.1209	0.1223
	3				0.1094	0.1108	0.1120	01213	0.1213	0.1225
90°	1	0.1	0.1	0.1	0.0765	0.0784	0.0796	0.1200	0.1200	0.12192
		0.5			0.0766	0.0784	0.07963	0.1201	0.12007	0.12193
		1			0.0767	0.0784	0.07965	0.1201	0.12009	0.12194
		2			0.0768	0.0785	0.07968	0.1201	0.1201	0.12196
90°	1	0.1	0	0.1	0.0874	0.0892	0.0905	0.0928	0.0928	0.0941
			0.05		0.0968	0.0989	0.1005	0.1060	0.1060	0.1076
			0.1		0.1069	0.1094	0.1111	0.1205	0.1205	0.12235
			0.2		0.1291	0.1325	0.1349	0.1542	0.1542	0.1568
90°	1	0.1	0.1	0.1	0.1069	0.1094	0.1111	0.1205	0.1205	0.12235
				0.5	0.3441	0.3705	0.3914	0.4590	0.4590	0.4871
				3	0.6420	0.3798	0.8264	1.1087	1.1087	1.2863
				10	0.7311	0.8593	0.9791	1.3836	1.3834	1.6706

5. Conclusions

By focusing on five different dimensionless parameters and involving two different types of magnetic nanofluids which are Fe_3O_4-water and Fe_3O_4-kerosene, the current study examines the effects of convective boundary conditions and the presence of a magnetic field on the behaviour of magnetic nanofluids by free convection flow passing over a different state of moving vertical plate. The following conclusion can be drawn based on the graphical and numerical results obtained:

i. The velocity profiles for both magnetic nanofluids increase as the value of α, M, Gr_x, and Bi_x increases, except ϕ.
ii. The temperature profiles for both magnetic nanofluids decrease as the value of α, M, and Gr_x increases, except ϕ and Bi_x.
iii. The value of skin friction coefficient and Nusselt number increases as the value of all dimensionless parameter increases.
iv. The skin friction coefficient of a moving plate against the flow is the maximum for all states of vertical plate, whereas the Nusselt number for a moving plate with magnetic nanofluids flowing is the highest.
v. Fe_3O_4-kerosene magnetic nanofluids have the highest heat transfer rate at the surface compared to Fe_3O_4-water in all states of vertical plate.

For future work, this model can be extended to hybrid nanofluids and different geometries configuration.

Acknowledgement
This research was supported by Universiti Teknologi MARA.

References

[1] Choi, S. US, and Jeffrey A. Eastman. *Enhancing thermal conductivity of fluids with nanoparticles*. No. ANL/MSD/CP-84938; CONF-951135-29. Argonne National Lab., IL (United States), 1995.

[2] Sandeep, N., and I. L. Animasaun. "Heat transfer in wall jet flow of magnetic-nanofluids with variable magnetic field." *Alexandria Engineering Journal* 56, no. 2 (2017): 263-269. https://doi.org/10.1016/j.aej.2016.12.019

[3] Gui, N. Gan Jia, C. Stanley, N-T. Nguyen, and G. Rosengarten. "Ferrofluids for heat transfer enhancement under an external magnetic field." *International Journal of Heat and Mass Transfer* 123 (2018): 110-121. https://doi.org/10.1016/j.ijheatmasstransfer.2018.02.100

[4] Zonouzi, Sajjad Ahangar, Rahmatollah Khodabandeh, Habibollah Safarzadeh, Habib Aminfar, Yuliya Trushkina, Mousa Mohammadpourfard, Morteza Ghanbarpour, and German Salazar Alvarez. "Experimental investigation of the flow and heat transfer of magnetic nanofluid in a vertical tube in the presence of magnetic quadrupole field." *Experimental Thermal and Fluid Science* 91 (2018): 155-165. https://doi.org/10.1016/j.expthermflusci.2017.10.013

[5] Sheikholeslami, Mohsen, Ahmed Zeeshan, and Aaqib Majeed. "Control volume based finite element simulation of magnetic nanofluid flow and heat transport in non-Darcy medium." *Journal of Molecular Liquids* 268 (2018): 354-364. https://doi.org/10.1016/j.molliq.2018.07.031

[6] Ghorbani, Babak, Sasan Ebrahimi, and Krishna Vijayaraghavan. "CFD modeling and sensitivity analysis of heat transfer enhancement of a ferrofluid flow in the presence of a magnetic field." *International Journal of Heat and Mass Transfer* 127 (2018): 544-552. https://doi.org/10.1016/j.ijheatmasstransfer.2018.06.050

[7] Kuznetsov, A. V., and D. A. Nield. "Natural convective boundary-layer flow of a nanofluid past a vertical plate: A revised model." *International Journal of Thermal Sciences* 77 (2014): 126-129. https://doi.org/10.1016/j.ijthermalsci.2013.10.007

[8] Mohamed, Muhammad Khairul Anuar, Nurul Ainn Ismail, Norhamizah Hashim, Norlianah Mohd Shah, and Mohd Zuki Salleh. "MHD slip flow and heat transfer on stagnation point of a magnetite (Fe3O4) ferrofluid towards a stretching sheet with Newtonian heating." *CFD Letters* 11, no. 1 (2019): 17-27.

[9] Ilias, Mohd Rijal, Nur Sa'aidah Ismail, Nurul Hidayah Ab Raji, Noraihan Afiqah Rawi, and Sharidan Shafie. "Unsteady aligned MHD boundary layer flow and heat transfer of a magnetic nanofluids past an inclined plate." *International Journal of Mechanical Engineering and Robotics Research* 9, no. 2 (2020). https://doi.org/10.18178/ijmerr.9.2.197-206

[10] Ilias, Mohd Rijal, Noraihan Afiqah Rawi, N. H. A. Raji, and Sharidan Shafie. "Unsteady aligned MHD boundary layer flow and heat transfer of magnetic nanofluid past a vertical flate plate with leading edge accretion." *ARPN Journal of Engineering and Applied Sciences* 13, no. 1 (2018): 340-351.

[11] Makinde, Oluwole D., and A. Aziz. "Boundary layer flow of a nanofluid past a stretching sheet with a convective boundary condition." *International Journal of Thermal Sciences* 50, no. 7 (2011): 1326-1332. https://doi.org/10.1016/j.ijthermalsci.2011.02.019

[12] Yao, Shanshan, Tiegang Fang, and Yongfang Zhong. "Heat transfer of a generalized stretching/shrinking wall problem with convective boundary conditions." *Communications in Nonlinear Science and Numerical Simulation* 16, no. 2 (2011): 752-760. https://doi.org/10.1016/j.cnsns.2010.05.028

[13] Alsaedi, A., M. Awais, and T. Hayat. "Effects of heat generation/absorption on stagnation point flow of nanofluid over a surface with convective boundary conditions." *Communications in Nonlinear Science and Numerical Simulation* 17, no. 11 (2012): 4210-4223. https://doi.org/10.1016/j.cnsns.2012.03.008

[14] Akbar, Noreen Sher, S. Nadeem, Rizwan Ul Haq, and Z. H. Khan. "Radiation effects on MHD stagnation point flow of nano fluid towards a stretching surface with convective boundary condition." *Chinese Journal of Aeronautics* 26, no. 6 (2013): 1389-1397. https://doi.org/10.1016/j.cja.2013.10.008

[15] Ibrahim, Wubshet. "The effect of induced magnetic field and convective boundary condition on MHD stagnation point flow and heat transfer of upper-convected Maxwell fluid in the presence of nanoparticle past a stretching sheet." *Propulsion and Power Research* 5, no. 2 (2016): 164-175. https://doi.org/10.1016/j.jppr.2016.05.003

[16] Goyal, Mania, and Rama Bhargava. "Simulation of natural convective boundary layer flow of a nanofluid past a convectively heated inclined plate in the presence of magnetic field." *International Journal of Applied and Computational Mathematics* 4, no. 2 (2018): 1-24. https://doi.org/10.1007/s40819-018-0483-0

[17] Mitra, A. "Computational modelling of boundary-layer flow of a nano fluid over a convective heated inclined plate." *Journal of Mechanics of Continua and Mathematical Sciences* 13, no. 2 (2018): 88-94. https://doi.org/10.26782/jmcms.2018.06.00006

[18] Ilias, Mohd Rijal, Noraihan Afiqah Rawi, and Sharidan Shafie. "Natural convection of ferrofluid from a fixed vertical plate with aligned magnetic field and convective boundary condition." *Malaysian Journal of Fundamental and Applied Sciences* 13, no. 3 (2017): 224-229. https://doi.org/10.11113/mjfas.v13n3.651

[19] Ilias, Mohd Rijal, Noraihan Afiqah Rawi, and Sharidan Shafie. "Steady aligned MHD free convection of Ferrofluids flow over an inclined plate." *Journal of Mechanical Engineering (JMechE)* 14, no. 2 (2017): 1-15.
[20] Alghamdi, Wajdi, Abdelaziz Alsubie, Poom Kumam, Anwar Saeed, and Taza Gul. "MHD hybrid nanofluid flow comprising the medication through a blood artery." *Scientific Reports* 11, no. 1 (2021): 1-13. https://doi.org/10.1038/s41598-021-91183-6
[21] Dinarvand, Saeed, Seyed Mehdi Mousavi, Mohammad Yousefi, and Mohammadreza Nademi Rostami. "MHD flow of MgO-Ag/water hybrid nanofluid past a moving slim needle considering dual solutions: an applicable model for hot-wire anemometer analysis." *International Journal of Numerical Methods for Heat & Fluid Flow* (2021). https://doi.org/10.1108/HFF-01-2021-0042
[22] Alblawi, Adel, Saba Keyani, S. Nadeem, Alibek Issakhov, and Ibrahim M. Alarifi. "Ciliary Flow of Casson Nanofluid with the Influence of MHD having Carbon Nanotubes." *Current Nanoscience* 17, no. 3 (2021): 447-462. https://doi.org/10.2174/1573413716999201015090335
[23] Abd Elazem, Nader Y. "Numerical results for influence the flow of MHD nanofluids on heat and mass transfer past a stretched surface." *Nonlinear Engineering* 10, no. 1 (2021): 28-38. https://doi.org/10.1515/nleng-2021-0003
[24] Krishna, M. Veera, and Ali J. Chamkha. "Hall and ion slip effects on MHD rotating flow of elastico-viscous fluid through porous medium." *International Communications in Heat and Mass Transfer* 113 (2020): 104494. https://doi.org/10.1016/j.icheatmasstransfer.2020.104494
[25] Krishna, M. Veera, and Ali J. Chamkha. "Hall and ion slip effects on MHD rotating boundary layer flow of nanofluid past an infinite vertical plate embedded in a porous medium." *Results in Physics* 15 (2019): 102652. https://doi.org/10.1016/j.rinp.2019.102652
[26] Zohra, Fatema T., Mohammed J. Uddin, and Ahamd IM Ismail. "Magnetohydrodynamic bio-nanoconvective Naiver slip flow of micropolar fluid in a stretchable horizontal channel." *Heat Transfer-Asian Research* 48, no. 8 (2019): 3636-3656. https://doi.org/10.1002/htj.21560
[27] Makinde, Oluwole Daniel. "Similarity solution for natural convection from a moving vertical plate with internal heat generation and a convective boundary condition." *Thermal Science* 15, no. 1 (2011): S137-S143. https://doi.org/10.2298/TSCI11S1137M
[28] Aziz, Abdul. "A similarity solution for laminar thermal boundary layer over a flat plate with a convective surface boundary condition." *Communications in Nonlinear Science and Numerical Simulation* 14, no. 4 (2009): 1064-1068. https://doi.org/10.1016/j.cnsns.2008.05.003
[29] Bataller, Rafael Cortell. "Radiation effects for the Blasius and Sakiadis flows with a convective surface boundary condition." *Applied Mathematics and Computation* 206, no. 2 (2008): 832-840. https://doi.org/10.1016/j.amc.2008.10.001
[30] Ishak, Anuar, Nor Azizah Yacob, and Norfifah Bachok. "Radiation effects on the thermal boundary layer flow over a moving plate with convective boundary condition." *Meccanica* 46, no. 4 (2011): 795-801. https://doi.org/10.1007/s11012-010-9338-4
[31] Ramesh, G. K., A. J. Chamkha, and B. J. Gireesha. "Boundary layer flow past an inclined stationary/moving flat plate with convective boundary condition." *Afrika Matematika* 27, no. 1-2 (2016): 87-95. https://doi.org/10.1007/s13370-015-0323-x
[32] Xuan, Yimin, and Qiang Li. "Investigation on convective heat transfer and flow features of nanofluids." *Journal of Heat Transfer* 125, no. 1 (2003): 151-155. https://doi.org/10.1115/1.1532008